Long-Range Intermolecular Interactions in Dilute Aqueous Solutions of Ionized Poly(L-lysine) at Low Ionic Strength

Katie R. Bruno and Wayne L. Mattice*

Department of Polymer Science, The University of Akron, Akron, Ohio 44325-3909

Received July 12, 1991

ABSTRACT: Measurements of nonradiative singlet energy transfer (Förster transfer) were performed to investigate the intermolecular interactions of ionized poly(L-lysine) in dilute aqueous solution at low ionic strength. The range of ionic strengths covered in the experiments includes the location of the "ordinary to extraordinary transition". Some of the molecules of the polymer were lightly labeled with donors, and others were lightly labeled with acceptors. Different combinations of labels, giving Förster radii ranging from 1.7 to 5.8 nm, were used. In the presence of low concentrations of added salt, enhanced efficiency for nonradiative singlet energy transfer was detected in the extraordinary regime only for the pair of labels that have the largest Förster radius. Measurements were also performed by dilution of the labeled species with unlabeled poly(L-lysine), at constant total concentration of polymer. A simple simulation was devised for interpretation of the rate of the decrease in the efficiency of Förster transfer upon substitution of unlabeled polymer for some of the labeled polymer. Comparison of the simulation with the experiment shows that each macromolecule "sees" only one or two other macromolecules, on the distance scale determined by the largest Förster radius, in the temporal aggregates that are formed in the "extraordinary" or low salt regime.

Introduction

The phenomenon described as the "ordinary to extraordinary transition" was first reported over 1 decade ago by Lin et al.[1] Dynamic light scattering was used to monitor the apparent diffusion coefficient of ionized poly(L-lysine) as a function of the concentration of added salt. The "transition" was detected as an increase, followed by a large decrease, in the apparent diffusion coefficient in a series of measurements performed with decreasing concentration of the added salt and constant concentration of the poly(L-lysine). Subsequently, this phenomenon has been detected by quasi-elastic light scattering with[2] and without[3,4] the presence of a sinusoidal electric field, low shear viscometry,[5] X-ray scattering,[6] electrophoretic light scattering,[7,8] and nonradiative singlet-energy transfer.[9]

There is no doubt about the existence of the phenomenon, but its molecular origin has not been conclusively established. Since the tracer diffusion coefficient as measured by fluorescence recovery after pattern photobleaching[8] is insensitive to the transition, the phenomenon cannot be attributed to increased polyion friction. A conformational transition would be dependent upon the molecular weight of the polymer, but the ordinary to extraordinary transition is independent of molecular weight.[10] The transition occurs for both cationic and anionic polyelectrolytes, is not specific to poly(amino acids), and is dependent on the valence, but not the type, of the added salt.

Drifford and Dalbiez[10] derived an empirical relationship which predicts the concentration of salt at which the transition will occur:

$$\frac{C_p}{\sum_i C_i Z_i^2 \xi} = Z_s \qquad (1)$$

where C_p is the concentration of the polymer, expressed in molarity of monomer units, $\sum C_i Z_i^2$ is the Debye screening of the added salt (species i, molarity C_i, valence Z_i), and ξ is the linear charge density parameter from Manning's theory.[11,12] This relationship has predicted reasonably well the concentration of salt at which the transition occurs in systems of either poly(L-lysine) or poly(styrene sulfonate).

Schurr and Schmitz[12] have proposed that the small diffusion coefficient in the extraordinary regime is due to short-term cooperative motion in regions of locally high macroion concentration, which they call "temporal aggregates". As salt is removed from a polyelectrolyte solution, the charge effect of each individual polyion extends farther into the solution. A continued reduction in the ionic strength eventually causes overlap of clouds of counterions from neighboring polyions. At this point the motion of the polyion and its associated counterions is coupled with the motion of neighboring polyions. The solution then contains regions of correlated polyion motions, where the local concentration of polyion is high and that of the counterion is depleted, and other regions of lower local concentrations, where the polyions behave independently. This situation produces a retardation of the relaxation of small local concentration gradients.

If the temporal aggregates that are responsible for the slow diffusion cause the molecules to approach one another to within a distance comparable with the Förster radius, denoted by R, nonradiative singlet-energy transfer (Förster transfer)[14] can be used to monitor the intermolecular interactions. Small-angle X-ray scattering measurements detect a peak at a position that implies an intermolecular distance of 6–10 nm.[6] Thus the pair of labels might require a value of R of 5 nm or greater if the temporal aggregates are to be detected by measurements of the fluorescence. If they can be detected, then additional information is accessible by taking advantage of the ability to dilute the labels, at constant concentration of polymer, by the substitution of unlabeled polymer for labeled polymer. This article reports the results of the measurements of the fluorescence for systems with several pairs of probes. A simple simulation is used to assist in the interpretation of the influence on the fluorescence of the replacement of some of the labeled polymer with unlabeled polymer.

Experimental Section

Materials. Poly(L-lysine) labeled with either fluorescein or rhodamine B was purchased from Molecular Probes. The supplier reported these samples had a viscosity average molecular weight of 15 000–30 000 and two or three probes per chain. The extent of labeling was verified by absorption measurements. The random copolymers poly(L-lysine-*co*-L-tryptophan) hydrobromide

0024-9297/92/2225-0327$03.00/0

(4:1) and poly(L-lysine-*co*-L-tyrosine) hydrobromide (4:1) were purchased from Sigma Chemical Co. The copolymers were reported to have a viscosity average molecular weight of 20 000–50 000. Unlabeled poly(L-lysine) with a molecular weight of 30 000 was also purchased from Sigma Chemical Co. The values of R for the donor:acceptor pairs tyrosine:tryptophan and tryptophan:rhodamine B are given as 1.7 and 2.8 nm, respectively, by Berlman.[15] A value of 5.6 nm was calculated for fluorescein:rhodamine B in glycerol.[16] The value of R increases to 5.8 nm when the solvent has the refractive index of water.

Measurements. A solution of poly(L-lysine) at the desired concentration was prepared using distilled deionized water. For the fluorescein:rhodamine B and tyrosine:tryptophan pairs, solutions were prepared with equal concentrations of donor and acceptor. For the tryptophan:rhodamine B pair an excess of tryptophan was used because it has a much smaller fluoresence quantum yield than rhodamine B.

Fluorescence was measured using a front-face cell and an SLM 8000C fluorometer equipped with a double monochromator in the excitation path. Excitation was at 468 nm for fluorescein:rhodamine B, which produces preferential excitation of the fluorescein. Excitation was at 278 nm for tyrosine:tryptophan, which preferentially excites the tyrosine. Finally, excitation was at 300 nm for tryptophan:rhodamine B, which preferentially excites tryptophan. The measurements of the emission were performed at 585 and 515 nm for fluorescein:rhodamine B, at 310 and 400 nm for tyrosine:tryptophan, and at 390 and 585 nm for tryptophan:rhodamine B. For each solution, the intensities were monitored 10 times, using an integration time of 10 s. These 10 measurements were used to compute the mean and the standard deviation of the mean.

The salt concentration was manipulated by addition in 0.025-mL aliquots of an aqueous solution of sodium choride. Although the concentration of poly(L-lysine) decreased slightly due to the addition of successive aliquots of aqueous sodium chloride, control measurements with the addition of deionized water showed little decrease in the efficiency of nonradiative singlet-energy transfer due to dilution alone.

For the fluorescein:rhodamine B system, the extent of Förster transfer, as defined by the ratio of the emission at 515 and 585 nm, was compared in the ordinary and in the extraordinary regime as a function of polymer concentration. Once the optimum concentration for observing the extraordinary regime was determined, the efficiency of nonradiative singlet-energy transfer was monitored as a function of the fraction of unlabeled polymer. To a labeled solution with no added salt, a solution of unlabeled poly(L-lysine) of the same concentration was added in 0.1–1.0-mL aliquots, and the emission at 515 and 585 nm was then measured.

Results When All Chains Bear Labels. The efficiency of nonradiative singlet-energy transfer was nearly independent of the concentration of added sodium chloride when the donor:acceptor pairs were tyrosine:tryptophan or tryptophan:rhodamine B, as shown in Figure 1 for the latter system. There is no evidence of a sharp change when the concentration of salt passes through the value associated with the ordinary to extraordinary transition. As reported previously,[9] there is a sharp change in the efficiency of nonradiative singlet energy transfer at about 0.01 M NaCl when the donor:acceptor pair is fluorescein:rhodamine B, as shown in Figure 2. There is enhanced Förster transfer at the lower concentration of salt. The location of the transition in Figure 2 is not as well-defined as in the original dynamic light scattering experiments,[1] but the location of the transition is in agreement with the prediction from eq 1.

The fact that the transition was detected only in the fluorescein:rhodamine B system, where the value of R is 5.8 nm, and was not detected in systems where R was 1.7 or 2.8 nm is consistent with the spacing of 6–10 nm calculated from X-ray scattering studies.[6] The inability to detect with transition when R is 2.8 nm shows that the association between the polyions does not involve close contact.

The ratio of the values of I_{585}/I_{515} at 0.1 M and 0.001 M NaCl provides an indication of the ease with which the transition can be measured at a particular concentration of polymer. Figure 3 depicts this ratio as a function of polymer concentration. The ratio decreases as the concentration of polymer increases from

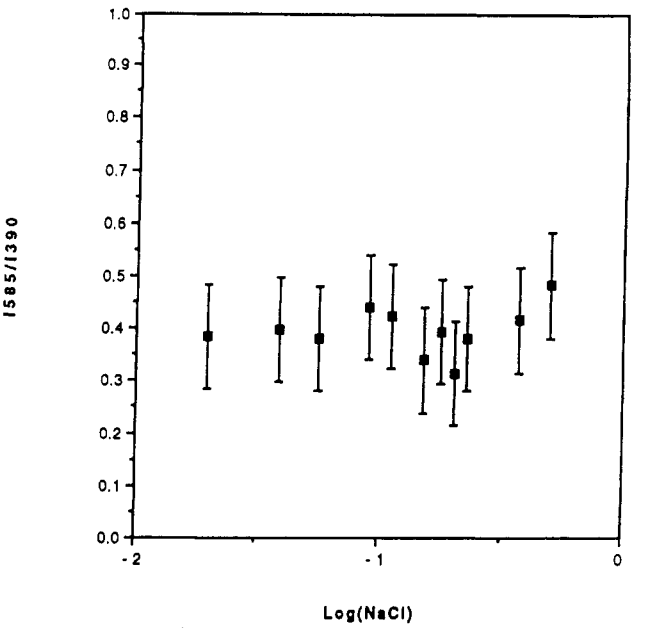

Figure 1. Ratio of the intensities of the emission at 585 and 390 nm when the donor:acceptor pair is tryptophan:rhodamine B.

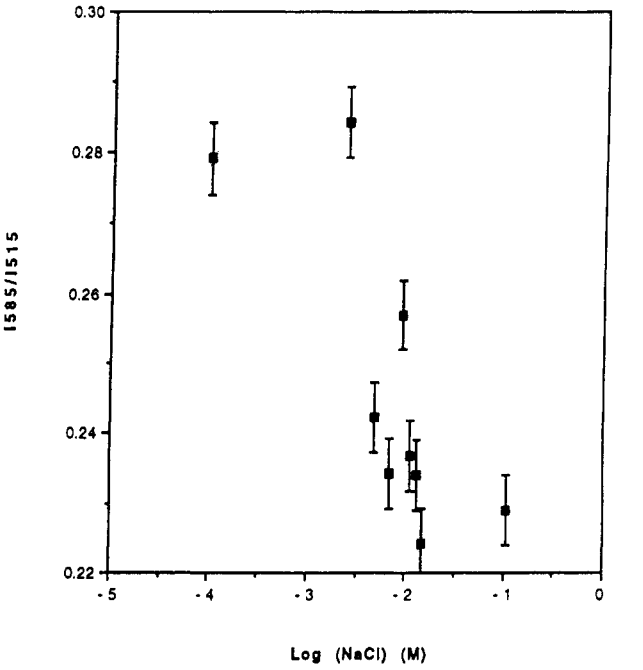

Figure 2. Ratio of the intensities of the emission at 585 and 515 nm when the donor:acceptor pair is fluorescein:rhodamine B.

0 to 1 mg/mL. Apparently fewer temporal aggregates are formed at the lower concentrations of polymer. The reversal of this trend as the concentration of polymer arises above 1 mg/mL may be an artifact due to reabsorption of light at high concentrations of the labels. The measurement is most sensitive to the transition when the concentration of polymer is 1 mg/mL.

Results When Labeled Chains Are Replaced by Unlabeled Chains. The points with the error bars in Figure 4 show how I_{585}/I_{515} in the fluorescein:rhodamine B system is affected by substitution of unlabeled (neat) polymer for labeled polymer. The total concentration of polymer is held constant at 1 mg/mL, and there is no added salt, so that the systems are in the extraordinary regime. The values of I_{585}/I_{515} have been scaled so that they range from 1, in the absence of neat polymer, to 0, in the absence of labeled polymer. The data show that I_{585}/I_{515} is nearly a linear function of the fraction of neat polymer. The interpretation of this result requires a simulation of the behavior expected for aggregates of different sizes.

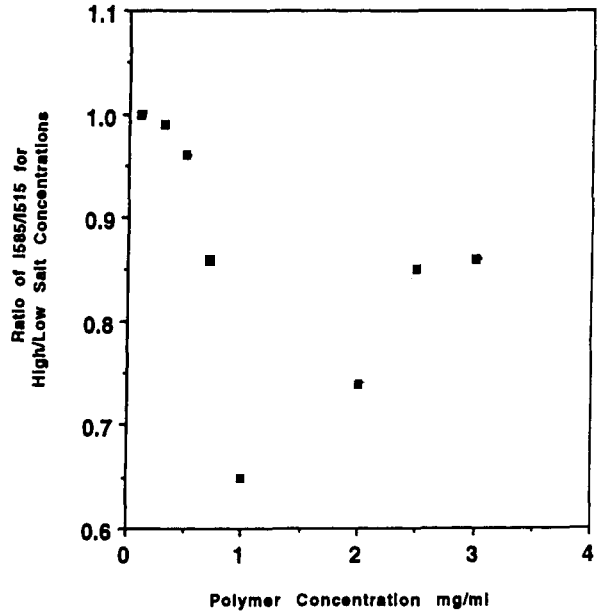

Figure 3. Ratio of the values of I_{585}/I_{515} at 0.1 and 0.001 M NaCl when the donor:acceptor pair is fluorescein:rhodamine B.

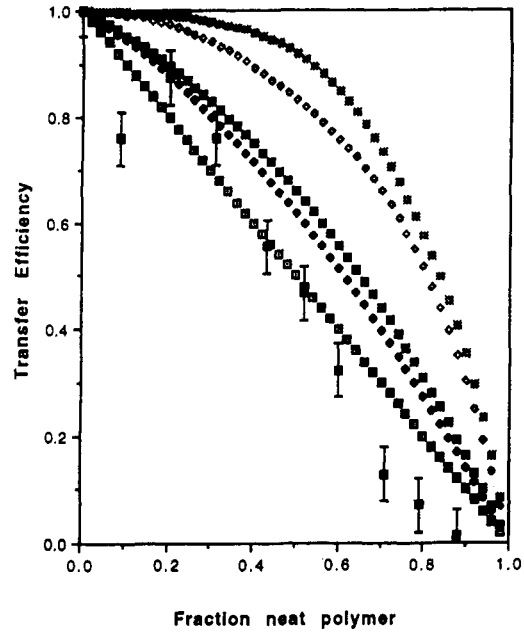

Figure 4. Comparison of the measured and simulated effects of neat polymer on the efficiency of Förster transfer. The points with error bars are I_{585}/I_{515}, scaled to run from an efficiency of 1 at no neat polymer to 0 at no labeled polymer. The curves without error bars are from simulations that assume aggregates are monodisperse and contain 2, 3, 4, 8, or 10 chains. Curvature in the calculated curves increases as the number of chains in the aggregate increases.

Simulations

Method. The simulation considers three species of polymer that are identical in every way except in their incorporation of labels. The three species are those labeled with donors (D), those labeled with acceptors (A), and those that are unlabeled (N). We assume Förster transfer will occur in any aggregate in which both D and A are present, and does not occur otherwise. The efficiency, E, of Förster transfer is defined in the simulation as

$$E = \frac{\text{number of D in an aggregate that contains at least one A}}{\text{total number of D}} \quad (2)$$

This definition assumes that D must transfer energy if an A is present in the same aggregate, and cannot transfer energy otherwise.

To calculate the value of E for an ensemble, the distribution of sizes for the aggregates must be specified. The calculation was performed for monodisperse distributions in which all chains were members of aggregates that contained 2, 3, 4, 5, 6, 7, 8, 9, or 10 chains. In the calculation for monodisperse aggregate sizes, we simply enumerate all possible combinations of D, A, N that will produce that size. The different aggregates of a specific size were weighted according to the degeneracy, evaluated under the assumption that all positions in the aggregate are equivalent. The mole fractions in the simulations obey the relationship

$$X_D = X_A = (1 - X_N)/2 \quad (3)$$

with X_N varying over the range 0–1, because this restriction was used in the experiments with which the results of the simulations will be compared. The calculation was also performed for various combinations of aggregates with different sizes, and for a continuous distribution of aggregate sizes. The continuous distribution assumes that the equilibrium constant for the addition of an isolated chain to an existing aggregate of m chains is independent of the value of m.

Simulations of Monodisperse Aggregates. The value of E, as defined by eq 2, is depicted as a function of X_N in Figure 5 for monodisperse aggregates of 2, 3, 4, 8, and 10 chains. In all cases, the value of E decreases as X_N increases. The curvature of the plots is strongly influenced by the sizes of the aggregates. Curvature is absent when the aggregates contain only two chains. Considering only those aggregates of two chains that contain at least one D, the species that produce energy transfer are AD and DA, and the species that contain D, but cannot transfer energy to another chain in the compex, are DD, DN, and ND. The value of E specified by eq 2 is therefore

$$E = (1 - X_N)/2 \quad (4)$$

which is linear in X_N.

As the size of the aggregates increases, the value of E at $X_N = 0$ also increases, because it is more likely that a D will be in an aggregate that contains at least one A. Furthermore, a larger value of X_N is required to produce a depression in E, causing an increasingly negative curvature as the size of the aggregates increases.

The computed curves for combinations of two discrete sizes of aggregates simply fall between the curves of the two aggregate sizes used in the combination. Therefore they all exhibit negative curvature. A small amount of a large aggregate is sufficient to produce noticable negative curvature in a system that is predominantly composed of aggregates of two chains. Negative curvature is also obtained if the aggregate sizes describe a continouous distribution.

Comparison of Experiment and Simulation

The curves depicted in Figure 5 can be normalized so that values of E range from 1 to 0 if each curve is divided by the value of E at $X_N = 0$. The normalized curves obtained in this manner from Figure 5 are plotted with the experimental results on Figure 4. The theoretical curve that provides the best fit to the data is the one that assumes that the aggregates contain only two chains. The two

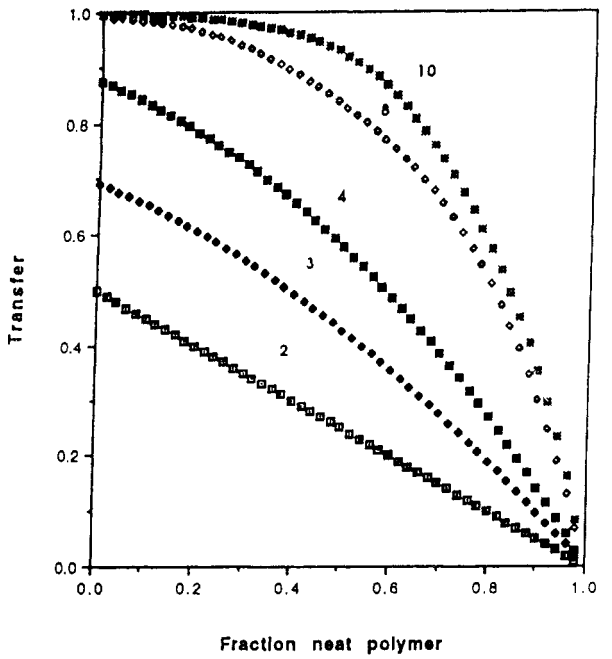

Figure 5. Calculated values of E from simulations that assume aggregates are monodisperse and contain 2, 3, 4, 8, or 10 chains.

experimental points obtained at $X_N = 0.2$–0.3 lie close to the line calculated for three chains per aggregate, but the great majority of points cannot support any curve other than the one which assumes an aggregate size of two chains. If the simulation postulates larger monodisperse aggregates, or polydisperse aggregates, the calculation will produce a result with negative curvature. Negative curvature is not supported by the experimental results. The most straightforward interpretation is that the "temporal aggregates" present in the extraordinary regime contain only two, or perhaps three, chains per aggregate.

None of the models produce the deviation from the straight line that is suggested by the three experimental points obtained with X_N in the range 0.7–0.9. If this deviation from linearity is real, it arises from a mechanism that is not encompassed in the simple simulation employed here.

The results might be made compatible with a larger aggregate size by assuming a special structure for the aggregate. Imagine, for example, an aggregate of n chains that is constructed so that no chain can "see" more than one or two of these chains, on a distance scale defined by R. This situation might occur if the n chains were assembled in a linear array, and arranged so that the spacing of next-nearest neighbors was much larger than R, but the spacing of nearest neighbors was on the order of R. Then internal chains in the linear array would "see" their two nearest neighbors, and the chains at the end of the linear array would "see" only their one neighbor. In terms of Figure 4, the expectation would lie between the curves computed for aggregates formed by two and three chains. Hence the experimental results can be compatible with an aggregate size larger than two or three chains, but only if the aggregate is structured such that a particular chain sees no more than one or two other chains, on the distance scale of R for the fluorescein:rhodamine B pair. That distance scale is 5.8 nm.

Acknowledgment. This research was supported by National Science Foundation Grant DMB 87-22238.

References and Notes

(1) Lin, S. C.; Lee, W. I.; Schurr, J. M. *Biopolymers* **1978**, *17*, 1046.
(2) Schmitz, K. S.; Ramsay, D. J. *Biopolymers* **1985**, *24*, 1247.
(3) Schmitz, K. S.; Lu, M.; Singh, N.; Ramsay, D. J. *Biopolymers* **1984**, *23*, 1637.
(4) Ramsay, D. J.; Schmitz, K. S. *Macromolecules* **1985**, *18*, 2422.
(5) Martin, N. B.; Tripp, J. B.; Shibata, J. H.; Schurr, J. M. *Biopolymers* **1979**, *18*, 2127.
(6) Ise, N.; Okubo, R.; Yamamoto, K.; Matsuoka, H.; Kawai, H.; Hishimoro, T.; Fujimura, M. *J. Chem. Phys.* **1983**, *78*, 541.
(7) Wilcoxon, J. P.; Schurr, J. M. *J. Chem. Phys.* **1983**, *78*, 3354.
(8) Zero, K.; Ware, B. R. *J. Chem. Phys.* **1984**, *80*, 1610.
(9) Bruno, K. R.; Mattice, W. L. *Polym. Commun.* **1989**, *30*, 310.
(10) Drifford, M.; Dalbiez, J. P. *Biopolymers* **1985**, *24*, 1501.
(11) Manning, G. S. *J. Chem. Phys.* **1969**, *51*, 924.
(12) Manning, G. S. *J. Chem. Phys.* **1969**, *51*, 3249.
(13) Schurr, J. M.; Schmitz, K. S. *Annu. Rev. Phys. Chem.* **1986**, *37*, 271.
(14) Förster, T. *Ann. Phys.* **1948**, *2*, 55.
(15) Berlman, I. B. *Energy Transfer Parameters of Aromatic Compounds*; Academic Press: New York, 1973.
(16) Kawski, A.; Kaminski, J.; Kuten, E. *J. Phys. B., At. Mol. Phys.* **1971**, *4*, 609.

Registry No. L-H-Lys-OH (homopolymer), 25104-18-1; L-H-Lys-OH (SRU), 38000-06-5; L-H-Lys-OH/L-H-Trp-OH (copolymer)·HBr, 137436-43-2; L-H-Lys-OH/L-H-Tyr-OH (copolymer)·HBr, 41705-04-8; NaCl, 7647-14-5.